Topographic setting of the Rio Grande rift, New Mexico: Assessing the role of flexural "rift-flank uplift" in the Sandia Mountains

Mousumi Roy, Karl E. Karlstrom, Shari Kelley, Frank Pazzaglia, and Steve Cather
1999, pp. 167-174. https://doi.org/10.56577/FFC-50.167

in:

Albuquerque Geology, Pazzaglia, F. J.; Lucas, S. G.; [eds.], New Mexico Geological Society 50 th Annual Fall Field Conference Guidebook, 448 p. https://doi.org/10.56577/FFC-50

This page is intentionally left blank to maintain order of facing pages.

TOPOGRAPHIC SETTING OF THE RIO GRANDE RIFT, NEW MEXICO: ASSESSING THE ROLE OF FLEXURAL "RIFT-FLANK UPLIFT" IN THE SANDIA MOUNTAINS

MOUSUMI ROY[1], KARL KARLSTROM[1], SHARI KELLEY[2], FRANK PAZZAGLIA[1], and STEVE CATHER[2]

[1]Department of Earth and Planetary Sciences, University of New Mexico, Albuquerque, NM 87131; [2]New Mexico Bureau of Mines and Mineral Resources, 801 Leroy Place, Socorro, NM 87801

Abstract—The Rio Grande rift is a north-trending system of grabens that formed as a result of Neogene extension along the eastern margin of the Colorado Plateau. The location of the rift coincides with the eastern edge of a zone of crustal thickening and high topography during the Laramide (Late Cretaceous–Eocene) orogeny. Following Laramide crustal thickening, the region may have undergone broad, epeirogenic uplift during mid-Tertiary time. This paper analyzes the topographic setting of the Rio Grande rift in order to the address the relative importance of Laramide shortening, mid-Tertiary epeirogeny, and Neogene extension in generating high topography and observed topographic variability along the rift. Flexural modeling of topography and gravity data within the Sandia Mountains suggests that much of the present-day short-wavelength topography of this mountain belt can be attributed to flexural footwall uplift in response to Neogene extension. Topographically high rift-flanks also exist, however, within hanging-wall blocks. These are not easily attributed to extension and, based on apatite fission-track dates, apparently reflect the combined effects of Laramide crustal thickening and mid-Tertiary regional denudation. Based on flexural modeling, together with geologic and geomorphologic arguments, we propose that extensional processes may have only locally modified topography along the Rio Grande rift. In particular, we argue that the broad, long-wave length (>1000 km) topographic high at the eastern margin of the Colorado Plateau (Alvarado ridge) probably post-dates Laramide crustal thickening and pre-dates the formation of the Rio Grande rift.

INTRODUCTION

The Rio Grande rift consists of a north-trending system of grabens that record Miocene–Quaternary extension at the eastern margin of the Colorado Plateau (Chapin and Cather, 1994). The crust in this region is strongly segmented and pervasively fractured along faults that record multiple episodes of Proterozoic to early-Tertiary tectonism, prior to the onset of extension in mid-Tertiary time (Karlstrom et al., 1999; this guidebook). Tectonics of the Rio Grande rift and its surroundings are thus influenced not only by Tertiary extension, but also by older deformational events. In particular, considerable controversy exists over the relative importance of Miocene–Quaternary extension and Mesozoic–Eocene (Laramide) tectonism in generating present-day topographic features of the Rio Grande rift, specifically the high-standing rift-flanks.

This paper examines the topographic setting of the Rio Grande rift in the context of "rift-flank uplift," or high topography generated as a flexural isostatic response to extensional unloading. Using simple models constrained by topography and gravity data, we assess the possible role of extension in generating regionally high-standing topography at the eastern edge of the Colorado Plateau and locally in the Sandia Mountains adjacent to the northern Albuquerque basin. We interpret these results in the context of uplift histories inferred from apatite fission-track data (Kelley et al., 1992; Kelley and Chapin, 1995, 1997), geologic data, and geomorphologic arguments (Pazzaglia and Kelley, 1998).

RIFT-FLANK UPLIFT

Although high topography in orogenic belts is generally attributed to isostatic compensation for crustal thickening during convergence, an important mechanism for generating high topography in extensional settings was recognized by Vening-Meinesz (1950). Topographically high mountains may be formed adjacent to extensional basins as a result of flexural response of the footwall to extensional unloading along normal faults (Fig. 1a–c; Vening-Meinesz, 1950; Wernicke and Axen, 1988). In weak lithosphere with no flexural rigidity (which corresponds to zero spring stiffness in Fig. 1a–b), we do not expect isostatic adjustments to lead to uplifted footwalls, and thus no "rift-flank uplift" can occur. In the simplest setting, where rifting breaks a region of low initial topographic relief, mountains formed by rift-flank uplift have a characteristically asymmetric shape, with steep faces towards the basin and broad gentle upwarps on the other side (Fig. 1c). The process of rift-flank uplift involves several types of "uplift," which are

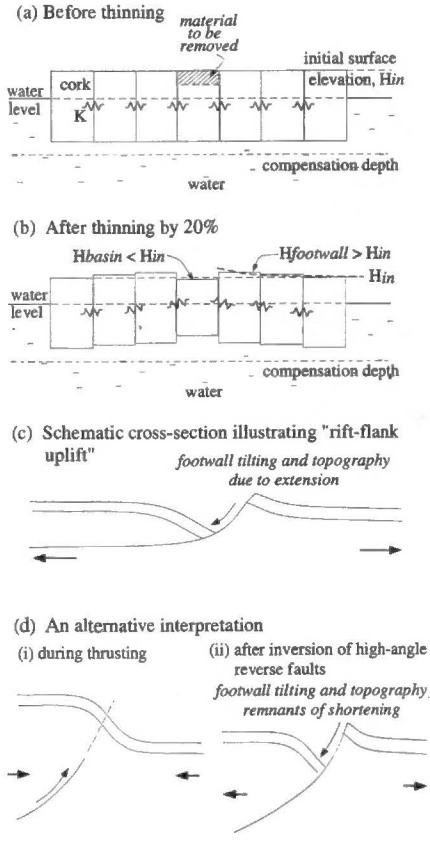

FIGURE 1. **a, b**, Cartoon model of rift-flank uplift. The elastic springs connecting the corks represent flexural rigidity of the "plate" made up of inter-connected corks. H_{in} is the initial elevation of the corks, and H_{basin} and $H_{footwall}$ are the post-thinning elevations of the basin and of the "footwall", respectively. For zero spring stiffness the corks move independently and there is no uplift of the "footwall" (corks adjacent to the central (thinned) one). **c**, Schematic diagram of the isostatic flexural response of the footwall unloaded by displacement on a listric normal fault. **d(i)**, Schematic diagram of tilting and upwarping of footwall rocks as a result of drag folds at a thrust fault or tilting at a monocline. **d(ii)**, Subsequent extension and exhumation of footwall rocks by fault inversion leads to similar final geometries as (c).

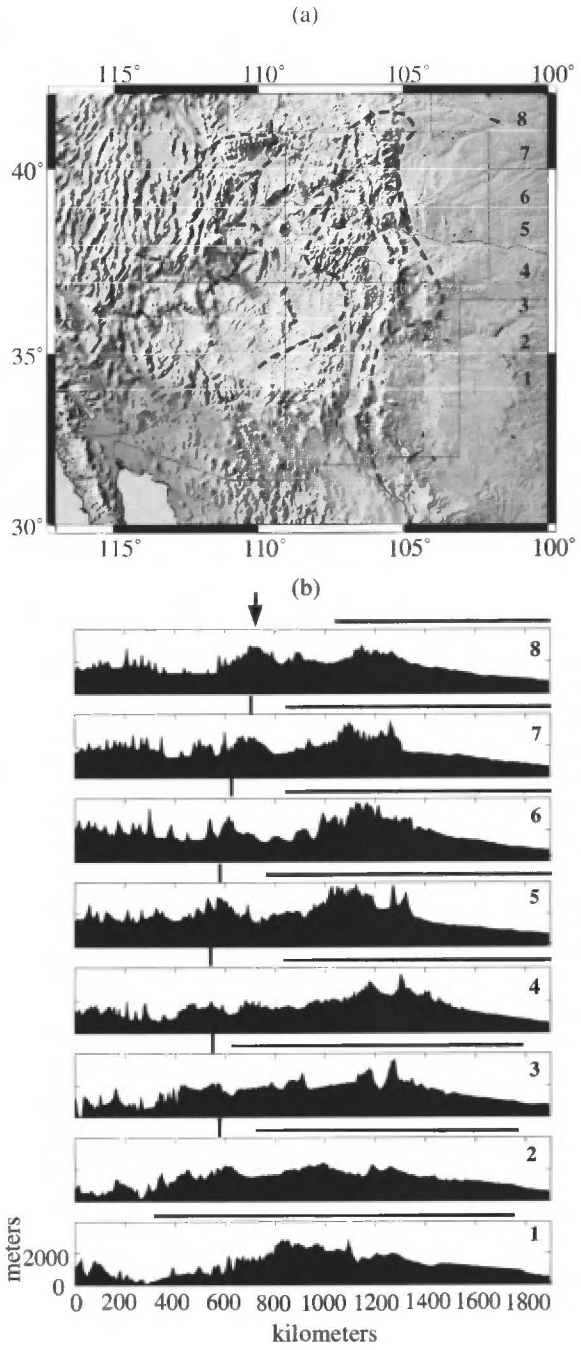

FIGURE 2. **a**, Topography of the Colorado Plateau region. The thick dashed lines enclose regions beneath which upper mantle seismic velocities (at 100 km) are reduced by 2% or more (modified from Humphreys and Dueker, 1994a, b; Karlstrom and Humphreys, 1998). Thin white lines indicate the locations of the E–W profiles in (b). **b**, East-west topographic profiles (smoothed) across the Colorado Plateau. The thick, horizontal black line in each panel roughly delineates the extent of Alvarado ridge in each profile. Alvarado ridge coincides spatially with the eastern zone of reduced seismic velocities in (a). The arrow and vertical lines indicate a prominent bulge at the western edge of the Colorado Plateau that coincides with the western region of reduced seismic velocities in (a). The axial basins of the Rio Grande rift form the central low on profiles 1–5. Profile 2 is a transect across the Sandia Mountains. Significant topographic features on other profiles include: a broad bulge corresponding to the Mogollon-Datil volcanic field (20–30 Ma) on profile 1, Jemez Mountains on the west and the Santa Fe Range on the east of the Rio Grande rift on profile 3, Sangre de Cristo Range on the East and the Tusas Range on the west of the rift on profile 4, the Wet Mountains and Sangre de Cristo Range on the east and the San Juan Range on the west of the rift on profile 5. Profiles 6 and 7 show the Colorado Rockies.

distinguished in the following discussion.

First, "surface uplift" is defined as the change in elevation of the land surface with respect to sea level. In the Sandia Mountains area, for example, surface uplift resulted from Laramide crustal thickening in the latest Cretaceous to early Tertiary, as rocks throughout the western U.S. went from at or below sea level to about 1–3-km elevation (Gregory and Chase, 1994).

Second, "rock uplift" is defined as the vertical translation of a parcel of rock relative to sea level. In isostatic equilibrium, this can occur by two processes: denudation, as fluvial erosion removes overburden and tectonic exhumation, as faulting brings rocks closer to the surface. The rate of rock uplift is therefore the sum of the surface uplift rate and the denudation and/or tectonic exhumation rate (Pazzaglia and Kelley, 1998). For the Cenozoic, one of our best gauges of the timing and rates of denudation (combined effects of tectonic exhumation and fluvial erosion) is apatite fission-track (AFT) data. These data reveal the time at which rocks cooled through 60–120°C (Kelley, 1990). In areas where magmatism or hydrothermal fluids are not important, AFT dates are often interpreted as recording the time at which rocks were unroofed to within 2–4 km of the surface.

"Rift-flank uplift," or flexural response to extension (Fig. 1a–c), involves tectonic exhumation of rocks in the footwall immediately adjacent to the normal fault. This process does not, however, cause tectonic exhumation of footwall rocks away from the fault. Therefore, flexural rift-flank uplift combined with variable degrees of erosional denudation of footwall rocks can lead to surface uplift in the footwall, and thus high-standing rift flanks. High topography within certain footwall blocks of the Rio Grande rift has been attributed to flexural rift-flank uplift (May et al., 1994), as discussed below.

TOPOGRAPHIC SETTING OF THE RIO GRANDE RIFT

Alvarado ridge

The Rio Grande rift is located along the culmination of a prominent, north-northeast trending, long-wavelength topographic high (wavelength >1000 km) at the eastern margin of the Colorado Plateau (Fig. 2). Following Eaton (1986), we refer to this feature as "Alvarado ridge." Possible models for the formation of Alvarado ridge include: (1) long-wavelength flexural rift flank uplift due to extension in the Rio Grande rift; (2) regional epeirogeny related to thermal buoyancy and passive asthenospheric upwelling driven by extension along the Rio Grande rift (Eaton, 1986); and (3) thermal buoyancy (and possibly dynamic support of topography) due to processes not caused by Rio Grande rift extension (in fact, these processes may have pre-dated and strongly influenced Rio Grande rift extension).

The first two interpretations, flexural uplift and passive upwelling, require a close genetic relationship between the amount and timing of extension in the axial basins of the Rio Grande rift (discussed below) and the formation of Alvarado ridge. In contrast, the third interpretation does not require the morphology of Alvarado ridge to be related to the magnitude of extension in the Rio Grande rift. Instead, the location of the thermal anomaly might have strongly controlled localization of extension in the Rio Grande rift. In the following section we show that although the topographic profile of Alvarado ridge is consistent with flexural uplift (albeit of a plate of unreasonably large rigidity), but the gravity data preclude such an interpretation. Instead, we argue below for a pre-rift, thermal origin for the high topography of Alvarado ridge.

As recognized by Eaton (1986), Alvarado ridge resembles the bathymetric profile of oceanic lithosphere as it cools and sinks away from a mid-ocean ridge (Fig. 2b). Although processes governing continental rifting do not involve lateral transport and cooling of lithosphere as in oceans, similar topographic profiles may be generated by mantle buoyancy modified by heat conduction away from a localized thermal anomaly. In this case, we expect elevation to decrease with distance from the anomaly (based on a modification of the half-space cooling model, e.g., Turcotte and Schubert, 1982). Topography of Alvarado ridge is well-matched by a simple square-root of distance function centered at the Rio Grande rift (hence the resemblance to a mid-ocean ridge; Fig. 3).

Based on this fit to the topography, we use a simple mass balance calculation assuming local isostatic compensation to infer density variations in the mantle lithosphere (Lachenbruch and Morgan, 1990). We find that, for a wide range of lithospheric thicknesses, the temperature at the base of the crust along the Rio Grande rift is about 1300–1400°C (Fig. 3). This simple analysis ignores regional compensation, dynamic topography, advective heat transport, chemical buoyancy of the mantle, and buoyancy due to the addition of basaltic melts; it is presented here only to suggest the possibility of a thermal origin of Alvarado ridge.

This interpretation is further supported by the fact that the axis of Alvarado ridge coincides with the location of a north-northeast-trending zone of low seismic velocities in the upper mantle (Fig. 2; Humphreys and Dueker, 1994a, b; Dueker, 1999, unpublished data). We also note a prominent topographic bulge at the western margin of the Colorado plateau that, interestingly, coincides with another zone of low upper mantle seismic velocities (Fig. 2; Humphreys and Dueker, 1994a,b; Dueker, 1999, unpublished data). These observations, together with recent studies that identify a significant contribution of mantle buoyancy to the elevation of the Colorado Plateau (Sheehan et al., 1995; Jones et al., 1996), suggest a thermal origin of the Alvarado ridge (see Discussion below).

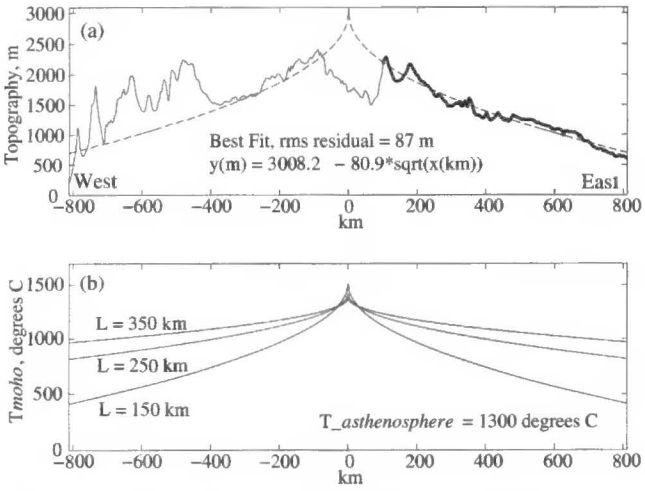

FIGURE 3. **a**, Best (polynomial) fit to smoothed topography of the eastern flank of Alvarado ridge at the latitude of the northern Albuquerque basin. The thick solid line indicates topography data used in the fitting procedure (smoothed version of profile 2 in Figure 2) and the dashed line is the fit. Note that although topography on the western flank of Alvarado ridge was not used in the fit, the best-fit line matches the western flank reasonably well. **b**, Using the best fit to the topography in (a), we follow the methods of Lachenbruch and Morgan (1990) to predict temperatures at the base of the crust. (We assume that the topography is statically supported by thermal buoyancy of the mantle, ignoring other effects (e.g., crustal thickness variations), and that the temperature at the base of the lithosphere is 1300°C.) Results are shown for a range of lithosphere thicknesses. All temperature profiles in (b) will produce the observed long-wavelength topography in (a).

Axial basins of the Rio Grande rift

The basins of the Rio Grande rift include (from north to south): the San Luis basin (east-tilted), Española basin (west-tilted), northern Albuquerque basin (east-tilted), and southern Albuquerque basin (west-tilted) (Fig. 4). (For simplicity, we divide the Albuquerque basin into two sub-basins, although recent work provides evidence for three sub-basins [Grauch et al., 1999, this volume].) These basins form a topographic low along the axis of Alvarado ridge and are locally flanked by

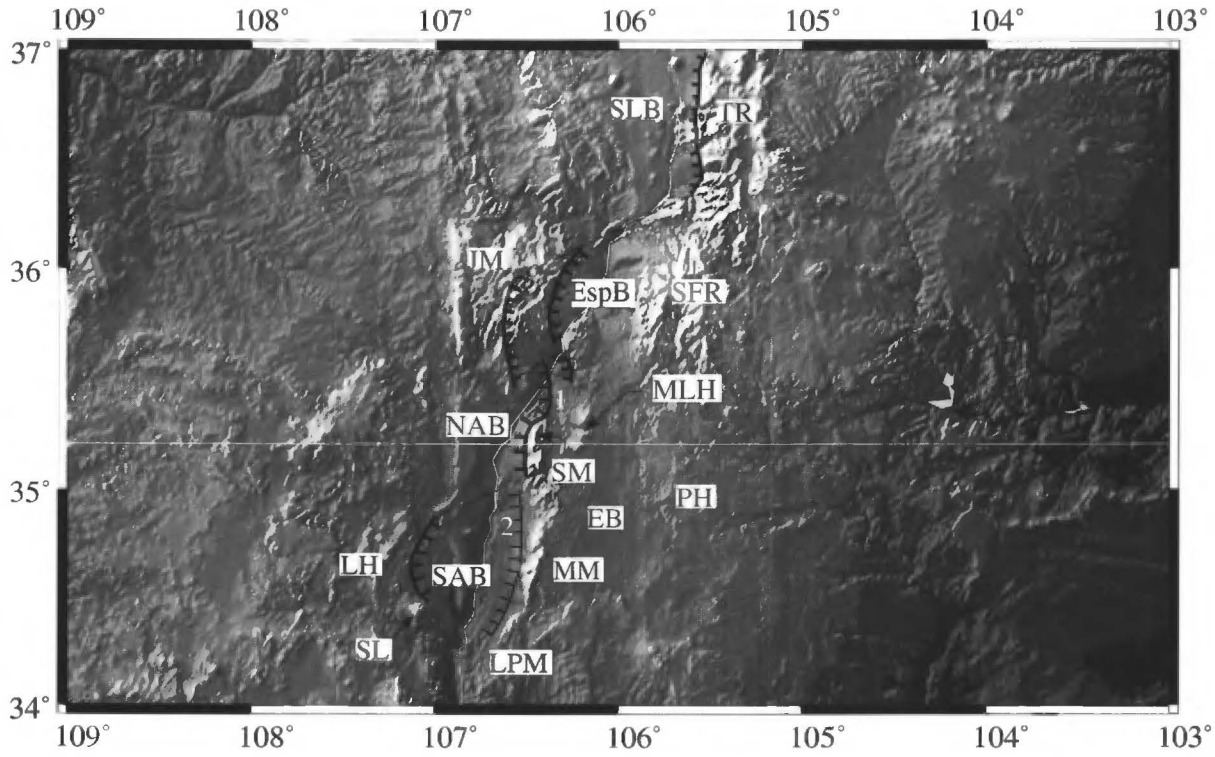

FIGURE 4. Shaded elevation map showing the locations of major extensional basins and adjacent topographic highs along the north-central Rio Grande rift. (Elevations are based on USGS 90-m resolution Digital Elevation Models, re-gridded to 30-second (1 km) resolution.) Axial Rio Grande rift basins include: San Luis basin (SLB), Española basin (EspB), northern Albuquerque basin (NAB), and southern Albuquerque basin (SAB). Topographically high rift-flanks: Taos Range (TR), Santa Fe Range (SFR), Jemez Mountains (JM), Sandia Mountains (SM), Manzano Mountains (MM), Los Pinos Mountains (LPM), Lucero Highland (LH) and Sierra Ladron (SL). To the east of the northern Albuquerque basin are the Monte Largo Hills (MLH), the Estancia basin (EB) and the Pedernal Hills (PH). East-west white line shows the location of the profile used in our flexural analysis. Thick black lines with barbs show approximate locations of master, basin-bounding normal faults with barbs on the down-dropped side (segment labeled 1 is the San Francisco fault). Thin black line with barbs is the Hubbell Bench, a normal fault that accommodates some east-tilting in the primarily west-tilted southern Albuquerque basin (the northern segment is labeled 2). Dashed lines show inferred locations of accommodation zones between oppositely tilted basins. Thin, wavy white line is the Rio Grande.

narrow linear asymmetric mountain belts (Figs. 2, 4). These rift-flank mountains include the Taos Range, the Santa Fe Range, the Sandia-Manzano-Los Pinos mountains, the Lucero highland, and Sierra Ladron (Fig. 4). The origin of these zones of high topography is controversial. Competing hypotheses include: (1) flexural rift-flank uplifts (for mountains within footwalls of the extensional basins) and (2) remnant highlands from Laramide crustal thickening (Fig. 1d; Karlstrom et al., 1999, this guidebook). We discuss below the strengths and weaknesses of these two hypotheses, primarily in the context of the Albuquerque basin.

Flexural rift-flank uplift has been suggested as a mechanism for generating asymmetric, topographically high mountains such as the Sandia Mountains and Sierra Ladron in the northern and southern Albuquerque basin, respectively. This interpretation is based on the correspondence of these zones of high footwall elevations and tilted fault blocks with youngest AFT dates, most rapid cooling, and thickest adjacent basin fill (May et al., 1994). For example, Chapin and Cather (1994) infer that rift-flank uplift resulted in deposition of the Ogallala Formation on the east flank of the Rockies and the Bidahochi Formation on the Colorado Plateau in middle Miocene to early Pliocene time. Therefore, assessing the nature and extent of these inferred Tertiary rift-flank uplifts is important for understanding the timing and tectonics of the Rio Grande rift.

Although the flexural rift-flank hypothesis is generally applied to the Sandias, there is considerable uncertainty in the details of this model. For example, it is not clear which fault is the master fault that accommodated extension and tilting of the footwall (Sandia-Rincon fault versus Rio Grande fault; Kelley and Northrop, 1975; Russell and Snelson, 1994). There is also uncertainty regarding the timing of motion and the dip on major extensional faults (25° from interpretation of regional seismic reflectors: Russell and Snelson, 1994; 75° for the San Francisco fault and most other related faults, based on surface dips: Menne, 1989). In addition, the rift-flank uplift model does not address perplexing observations, such as the presence of high-elevation rift flanks within hanging wall blocks of the master faults (e.g., the Santa Fe Range east of the Española basin; Fig. 4) and the absence of high elevations in footwall blocks along some segments of master faults (e.g., the northern Hubbell bench and San Francisco fault in the northern Albuquerque basin; Fig. 4). It seems likely that flexural uplift will be more pronounced in areas with a single master fault and an asymmetric basin (e.g., northern Albuquerque basin, San Luis basin) than in areas where extension is distributed across several faults (western side of Española basin), or where extension is more symmetrical (southern Albuquerque basin).

As an alternative to the flexural rift-flank uplift model, it has been suggested that some of the high topography of the rift-flanks may reflect a Laramide ancestry of crustal thickening and surface uplift within the region (Karlstrom et al., this volume). This may be an explanation for the topographically high Santa Fe Range (Fig. 4), which is within the hanging wall block, where AFT data suggest Laramide exhumation (Kelley et al., 1992). Also, the asymmetric topographic profile of the Sandia Mountains may be interpreted as reflecting the initial tilts of broad, Laramide monoclines (Fig. 1d). Karlstrom et al. (this volume) suggest that earlier tectonism may have also influenced fault geometries within the rift. For example, present-day extension is accommodated primarily by the inversion of steep Laramide thrust faults, and the right-stepping of the graben system reflects the geometry of Laramide transpressional faults.

Apatite fission-track cooling dates for rocks at the top of the Sandia Mountains are about 30 Ma, with mean track lengths of 14.5–15.0 μm (Kelley et al., 1992). These data indicate that this region cooled through 60–120°C by 30 Ma, as rocks were brought to within 2–4 km of the surface, probably by fluvial erosion. Rocks from low elevations give fission-track dates of ca. 14 Ma, and suggest that rock uplift was active through much of the Miocene.

In contrast, AFT dates from the top of the Manzano Mountains are older, ca. 40 Ma, with shorter mean track lengths of 12.8–13.8 μm (Kelley et al., 1992). This suggests that this area cooled more slowly (denuded to within 2–4 km of the surface) some 10 m.y. earlier than the Sandias. The Los Pinos Mountains yield Laramide-age AFT-cooling dates. In the context of the flexural rift-flank uplift model, the observation of younger AFT cooling dates within the Sandias relative to the Manzanos may be interpreted as evidence for high topography in the Manzano-Los-Pinos Mountains since Laramide time, and uplift of the Sandia Mountains in Miocene time in response to extension (May et al., 1994). In contrast, these observations may be explained in the context of an alternative model (which ascribes some rift-flank topography to Laramide crustal thickening) by invoking differential erosion (denudation) rates (Karlstrom et al., this volume). In either case, differential N–S denudation along the Sandia-Manzano-Los Pinos Mountains is required, with greater denudation to the south during Laramide deformation and greater denudation to the north prior to and during Rio Grande rift extension (Karlstrom et al., this volume).

The discussion above illustrates the need to assess the relative importance of Laramide crustal shortening vs. Tertiary extension in generating topographically high rift-flanks in the Rio Grande rift. The Albuquerque basin is an excellent place to evaluate these processes, as there are reasonably good seismic and well-log data within the basin (e.g., Russell and Snelson, 1994), a preserved record of syn-rift sedimentation (e.g., Lozinsky, 1994), a good fission-track data base (Kelley et al., 1992; Kelley and Chapin, 1995; Kelley and Chapin, 1997; Pazzaglia and Kelley, 1998), and a relative scarcity of syn-extensional magmatism.

FLEXURAL RIFT-FLANK UPLIFT IN THE SANDIA MOUNTAINS

In this section, we use a simple flexural model in conjunction with topography and gravity data in the Sandia Mountains region to assess the role of Tertiary extension in generating present-day topography. The modeling technique is based on Kruse and Royden (1994) and Roy et al. (1996), and involves a joint-inversion of topography and gravity data for plate flexure. For simplicity, we assume flexure of a uniform rigidity plate rather than considering a plate with laterally varying rigidity, although future models could incorporate changing rigidity (e.g., Roy et al., 1996).

Alvarado ridge

Although the long-wavelength topography of Alvarado ridge is consistent with thermal uplift (Fig. 3), we can also test the hypothesis that it is a flexural response to extension. We consider one-sided deflection of a uniform rigidity plate, with the plate end located at the topographic crest of the Sandia Mountains. The topographic profile of Alvarado ridge agrees with plate deflection for rigidities in the range of $D = 1–7 \times 10^{24}$ Nm, or effective elastic thickness of $T_e = 60–100$ km (Fig. 5). (In the rest of the paper, we refer interchangeably to the terms "flexural rigidity", D, and "effective elastic thickness," T_e, where we assume a Young's modulus of $E = 8.1 \times 1010$ Pa and $\nu = 0.25$ for Poisson's ratio.) Deflection of a plate of $T_e < 60$ km does not fit the topography of Alvarado ridge, as the flexural wavelength is too short. One feature of all these fits is that, although the general form of the long-wavelength topography is matched, they underestimate the slope and height of the linear, asymmetric Sandia Mountains on the eastern flank of the Albuquerque basin.

For the calculations above, the topography and gravity data are used jointly as constraints in a least-squares inversion for plate flexure (Kruse and Royden, 1994; Roy et al., 1996). Although the topography can be matched, the corresponding predicted gravity signal, however, does not match the observations (Fig. 5). We conclude that the regional topography is not flexural in nature. (It is important to note, therefore, that analyses of topography alone [e.g., Brown and Phillips, 1997] are insufficient to constrain flexural responses.) The conclusion that regional topography is not of flexural origin is further supported by the observation that the isostatic gravity anomaly (observed Bouguer anomaly minus the predicted Bouguer anomaly for Airy compensation) is negative along much of the eastern flank of Alvarado ridge (Fig. 5).

This implies a mass deficit within the lithosphere and is consistent with increasing thermal buoyancy towards the axis of Alvarado ridge.

Total (Paleozoic to Cenozoic) flexure in the Sandia Mountains

As flexural uplift does not explain the regional topography of Alvarado ridge, we now investigate the possibility that the Sandia Mountains represent shorter wavelength flexural uplift in response to extension. Topographic profiles across the Sandias show a steep, west-facing basinward flank and a broad, gently sloping eastern flank (Fig. 6a; profile location in Fig. 4). The eastern flank of the Sandias is essentially the dip slope of the Pennsylvanian Madera Group, the base of which crops out near the topographic crest of the mountains (Fig. 6b). The Madera Group is constrained by seismic reflection and well-log data to be at depths between 500–1800 m in the adjacent Estancia basin (Barrow and Keller, 1994; Broadhead 1997). At the latitude of our profile, the Estancia basin is a broad, shallow syncline, with <150 m of Tertiary sediments (Broadhead, 1997). Between the Sandia Mountains and the Estancia basin are the Monte Largo Hills (Fig. 6a), within which Precambrian rocks are uplifted along faults that have little or no late-Tertiary dip slip motion (thought to be of Laramide ancestry; see AFT data in Abbott, 1995). We assume in this paper that prior to flexure, the Madera Group is initially flat outside of pre-existing downwarps (in the San Pedro syncline [Fig. 6b] and the Estancia basin) and a local uplift at the Monte Largo Hills. In the flexural interpretation, the warping of the base of the Madera on the east flank of the Sandia Mountains, therefore, represents the total flexure of the region accumulated since Paleozoic time. As topography on the eastern flank of the Sandias mimics the base of the Madera Group (Fig. 6b), we use the elevation of the eastern flank as a proxy for plate deflection in this region.

Thus, topography of the east flank of the Sandia Mountains and gravity data are used to constrain deflection of an initially flat elastic plate (which may have had non-zero initial elevation). Within the San Pedro syncline and the Estancia basin (Figs. 4, 6) there are no constraints on plate deflection. Here, the elevation of the base of the Madera Group represents the combined effects of pre-existing geometry and possible flexure. Similarly, within the Pedernal Hills and to the east (Figs. 4, 6), there are no constraints on plate deflection. In particular, the relationship between topography in this region and possible flexure in the

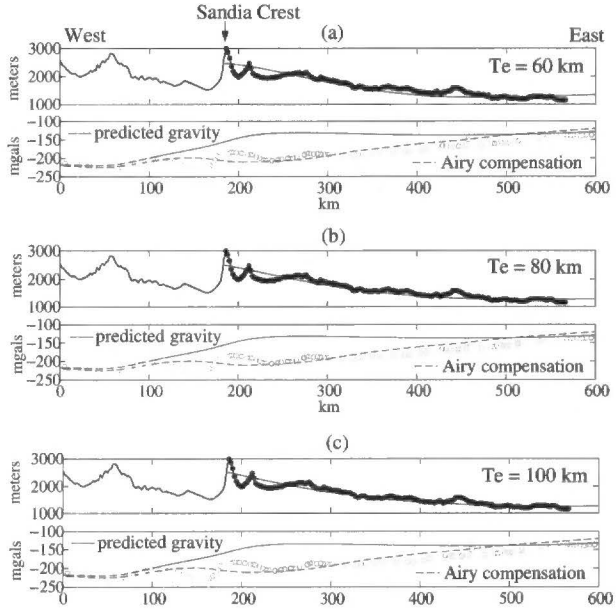

FIGURE 5. **a–c**, Joint-inversion of topography and gravity data to find the best-fit flexural profile along the eastern flank of Alvarado ridge at the latitude of the northern Albuquerque basin (profile location in Figure 4). Upper panel: Topography data (solid dots) and best flexural fit (thin solid line). Lower panel: Observed gravity data (open circles), predicted gravity from flexural solution (thin solid line) and predicted gravity in Airy compensation (thin dashed line). Results are shown for effective elastic thickness T_e = 60 km (a), T_e = 80 km (b), and T_e = 100 km (c). Regional reduced Bouguer gravity was obtained from G. R. Keller (personal comm., 1999).

Sandia Mountains is unknown. For simplicity, we assume that topography east of the Estancia basin represents a combination of flexural effects (to be modeled) and initial, pre-existing topography on the plate. Thus, using the predicted plate deflection in this region (obtained from gravity and topography data), we can infer the initial topography on the plate (initial topography = observed topography minus plate deflec-

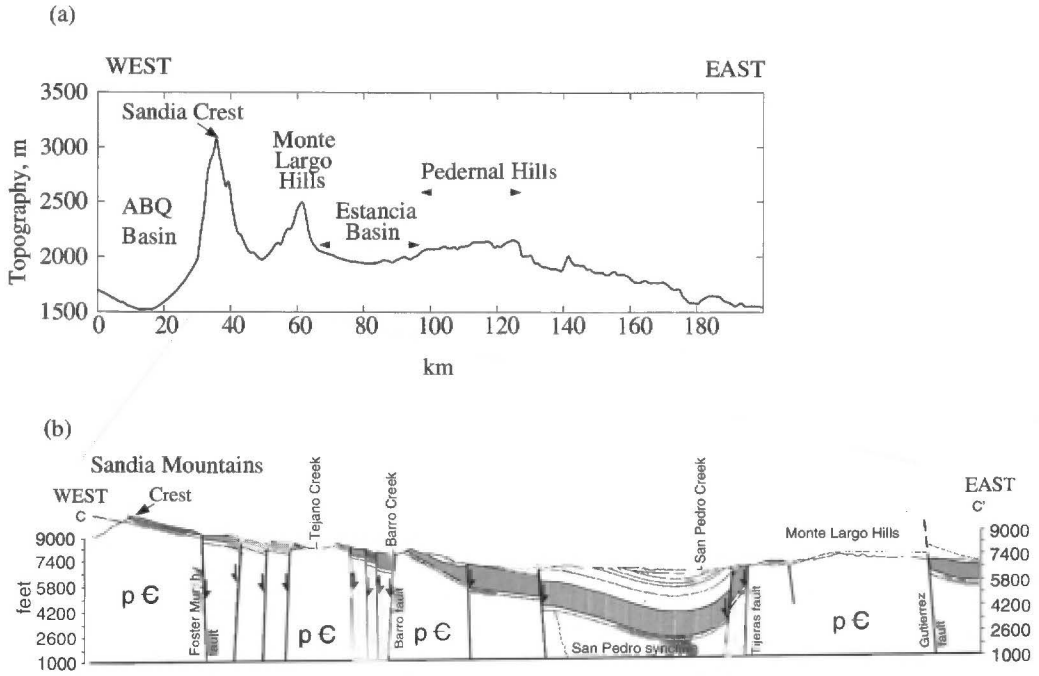

FIGURE 6. **a**, Topographic profile across the Sandia Mountains with locations of topographic features indicated (profile location in Fig. 4). **b**, An interpreted geologic cross-section emphasizing the locations of Paleozoic to Mesozoic strata in the Sandia Mountains and Monte Largo Hills to the east (modified from Kelley, 1975). Shaded band indicates the Paleozoic Madera Group.

tion).

A broad range of possible fits to the deflection and gravity data along the eastern flank of the Sandia Mountains exists (Fig. 7). The best fit to the deflection and gravity data is obtained for a plate of effective elastic thickness of 5 km, at an initial elevation of about 1640 m. Note that very low plate rigidities are required locally to fit the deflection data in the Sandias, however, these results do not constrain flexural rigidities further to the east. The inferred initial topography for the best-fitting plate flexure (T_e = 5 km) coincides with present-day topography east of the Pedernal Hills (Fig. 7b), consistent with the possibility that regionally high elevations related to Alvarado ridge pre-date Rio Grande rift extension. The best-fitting flexural rigidity ($D = 9 \times 10^{20}$ Nm) and effective elastic plate thickness (T_e = 5 km) are consistent with values obtained in other extensional regions with high heat flow, and may represent thermal weakening of the plate near the Rio Grande rift (e.g., Block and Royden, 1990; Roy et al., 1996).

We conclude, therefore, that warping of the Madera Group, and thus topography of the eastern flank of the Sandias, is consistent with flexure in response to vertical isostatic loads due to extensional unloading. We observe that the best-fitting plate flexure (T_e = 5 km; Fig. 5) also requires downwarping (~600 m) within the Estancia basin, so that present-day elevations of the Madera Group here are a combination of flexure and pre-existing faulted geometries. We suggest that the predicted downwarping of the Estancia basin might explain the observation of Quaternary sedimentation in the basin without Quaternary motion on the basin-bounding faults. This interpretation quantifies the association between downwarping in the Estancia basin and uplift of rift flanks noted by Chapin (1971).

As a test of our flexural interpretation, we now use the method in Roy et al. (1996) to infer the amount of crustal thinning in the Albuquerque basin and compare this isostatic load to that required for the best-fitting plate flexure. We calculate the deflection of a 5-km-thick elastic plate that is initially at 1640 m (as above), and extends from the crest of the Sandias westward across the Albuquerque basin. This plate is constrained to match the topographic height and slope at the crest of the Sandias and constrained to have zero deflection to the west of the Albuquerque basin (Fig. 8). The calculated deflection of this plate, minus the observed topography, provides an estimate of the amount of material removed by crustal thinning (Fig. 8b; note that the present-day basin-fill is not included in this calculation). The isostatic response can thus be restored to infer the amount of crustal thinning in the northern Albuquerque basin, about 2 km of maximum thinning in Figure 8a (18% horizontal change in line length). This estimate of thinning is somewhat lower than the 5–10-km values inferred from crustal thickness variations farther to the south (Keller et al., 1998), and probably reflects increasing magnitude of extension from north-to-south along the Albuquerque basin (Chapin and Cather, 1994). The total (upward) vertical load represented by this thinning is estimated to be about 2 x 10^{12} Nm^{-1} (from the shaded area in Fig. 8, using crustal density of 2670 kg/m^3). The extensional load required for the best-fitting flexural profile in Fig. 7b is about 4 x 10^{12} Nm^{-1}, which is slightly larger than, but of the same order of magnitude as the load estimated above. The agreement between the estimated load due to crustal thinning and the load required for the best-fitting plate flexure suggests that present-day topography in the Sandias is consistent with flexure in response to Neogene extension in the Albuquerque basin.

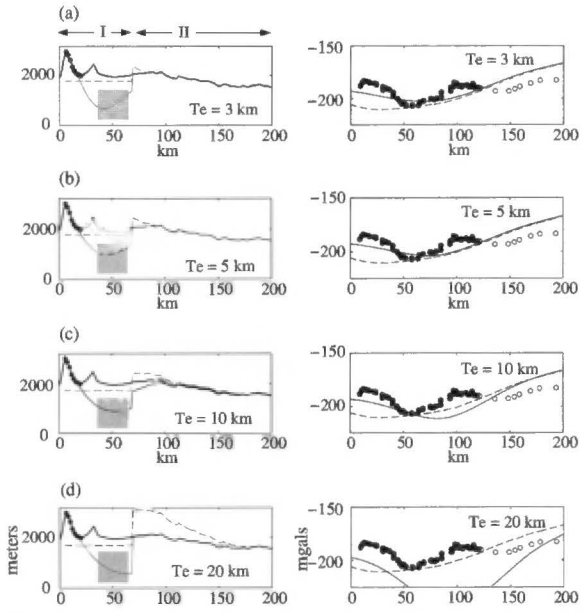

FIGURE 7. Fits to deflection (topography) and gravity data along the eastern flank of the Sandia Mountains and in the Estancia basin (profile location – white line on Fig. 4). The effective elastic plate thickness is indicated in each panel. Left panels: Topography (black solid line), deflection data (dots), calculated plate deflection (thin gray line) and estimated initial elevations (dashed line). Shaded region indicates the depths occupied by the Madera Group in the Estancia basin south of this profile (Barrow and Keller, 1994). In region I, we assume that the plate is initially flat and solve for the best-fitting initial elevation (dashed line). In region II, we assume that present-day topography is a sum of flexural deflection (thin gray line) and pre-existing topography (dashed line). Note that where the inferred initial topography (dashed line) merges with present-day topography, there is no predicted flexural deflection. Right panels: Observed Bouguer gravity data not used in the inversion (open circles), Bouguer data used in inversion (solid dots), calculated fit to the Bouguer signal (solid line), and predicted Bouguer signal for Airy compensation (dashed line).

DISCUSSION

The results above suggest that the present-day topography of the Sandia Mountains can be largely attributed to rift-flank uplift in response to Neogene extension in the Rio Grande rift. This conclusion depends, however, on our simplistic assumption that the base of the Madera Group was initially flat on the eastern flank of the Sandias, i.e. assuming that faults on the eastern flank have little or no late Tertiary dip-slip motion. The validity of our assumption remains to be tested in future work. The analysis above also suggests that the broader, long-wavelength topography of Alvarado ridge is not flexural in origin, so that flexural uplift may be important only locally, immediately adjacent to the Rio Grande rift.

The relative importance of Tertiary flexural uplift remains equivocal,

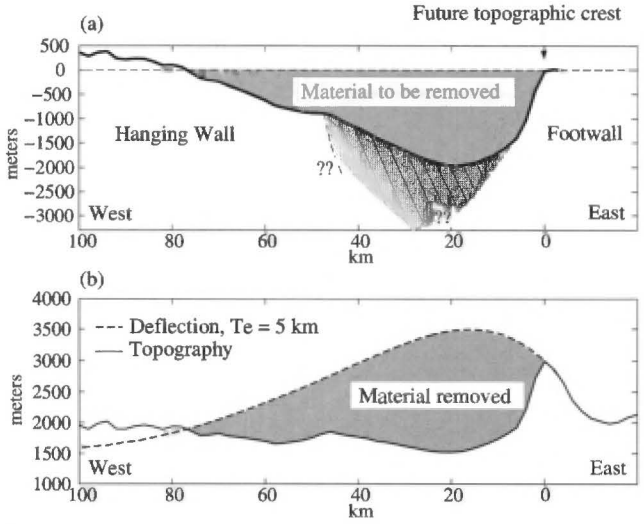

FIGURE 8. **a**, Estimate of the material removed from the northern Albuquerque basin (shaded region) above a west-dipping normal fault adjacent to the Sandia Mountains, as described in the text (based on Roy et al., 1996). This reconstruction neglects isostatic response to unloading, giving the pre-faulting geometry. Cross-hatched area shows the approximate extent of preserved basin sediments at the latitude of our profile (Fig. 4), based on line 50 of Russell and Snelson (1994). Note that these sediments are shown only for illustration; the present-day basin geometry is not used in any of our calculations. **b**, Same as (a), but with the isostatic response to unloading included.

however, in the context of significant, topographically high rift flanks within hanging wall blocks (for example, the Santa Fe Range east of the Española basin) and the absence of high topography in the footwalls of major extensional structures (for example, the San Francisco fault in the Albuquerque basin, north of the Sandias). Therefore, topographically high mountains within hanging wall blocks, such as the Santa Fe Range and the Manzano Mountains, may reflect a large component of rock and surface uplift due to Laramide crustal thickening and/or mid-Tertiary epeirogeny (discussed below).

We now turn to the possible relationships between local, rift-flank uplift along the Rio Grande rift and the regional topography of Alvarado ridge. It is interesting to note that the topographic signature of Alvarado ridge extends northward along the eastern edge of the Colorado Plateau, beyond the northern extent of significant Rio Grande rift extension (Fig. 2b). We suggest, therefore, that the topography of Alvarado ridge is not due to passive asthenospheric upwelling in response to Rio Grande rift extension. Instead, this broad topographic feature may be due to thermal (or chemical) buoyancy pre-dating formation of the Rio Grande rift. This interpretation is supported by the observation that total extension in the Rio Grande rift (maximum 25% in the northern Albuquerque basin and about 50% in the vicinity of Socorro) is unlikely to generate the sustained passive asthenospheric upwelling required to produce the inferred thermal buoyancy in the lithosphere (Fig. 3).

Our flexural analysis is consistent with the idea that the topography of Alvarado ridge pre-dates Rio Grande rift extension. The results above suggest that if Tertiary flexure due to extension is responsible for high topography in the Sandias, then the initial, pre-rift elevation of the region was about 1600 m. In addition, the best-fitting flexural curve does not require significant deflections east of the Estancia basin, suggesting that: (1) flexure adjacent to the Rio Grande rift is of short wavelength and (2) topography east of the Estancia basin may have predated Rio Grande rift extension. Together with the observation that the regional topography of Alvarado ridge is not flexural in origin, these results suggest that thermal uplift and the formation of Alvarado ridge may have pre-dated extension in the Rio Grande rift. This idea is discussed below in the context of regional denudation of the southern Rocky Mountains.

Regional denudation of the Southern Rocky Mountains and Alvarado ridge

Crustal thickening during the Laramide orogeny was accompanied by the uplift of mountain ranges and syn-tectonic subsidence of basins. Detritus from uplifting ranges was shed into over-filled syn-tectonic basins and spilled out as a broad eastward-tapering subaerial wedge across the High Plains and into the Gulf Coast. The result was a protracted period of pedimentation of mountain fronts, favored by stable (or locally rising) base level in the adjacent basins. Widespread erosion surfaces in the Southern Rocky Mountains (the Rocky Mountain surface of Chapin and Kelley [1994], or Eocene erosion surface of earlier authors) attest to this period of fluvial reduction of relief. Paleobotanical data suggest that at the end of Eocene time, the Southern Rocky Mountains stood, on average, about 2.5 km above sea level (Chase et al., 1998). By the late Oligocene (~30 Ma), the paleobotanical data suggest an increase in mean elevation to almost 4 km (Chase et al., 1998). In addition, late Oligocene to early Miocene AFT dates in the eastern Sangre de Cristo Mountains and on the High Plains of northeastern New Mexico also indicate regional-scale denudation at this time, extending from the Wet Mountains of southern Colorado south into New Mexico (Kelley and Chapin, 1995). The timing of this regional denudation event coincides with the exhumation of Oligocene intrusive rocks such as Sierra Blanca, the Capitan pluton, and the Spanish Peaks. No appreciable crustal thinning and extension is documented during this time in New Mexico, and the increase in mean elevation appears to predate the formation of the Neogene Rio Grande rift.

We attribute the topographic signature of Alvarado ridge in New Mexico and southern Colorado to rock and surface uplift associated with a combination of Laramide crustal thickening and late Oligocene to early Miocene regional denudation. The timing of the mid-Tertiary regional denudation in the vicinity of the Rio Grande rift coincides with 20–35-Ma magmatism in New Mexico and southern Colorado (e.g., in the San Juan Mountains, the Taos Range, and Mogollon and Datil volcanic fields). Interestingly, Laramide age AFT dates (50–70 Ma) in northern Colorado coincide with similar age magmatism in the Colorado mineral belt. Thus, the topography of Alvarado ridge may have a composite origin, resulting from diachronous introduction of thermal buoyancy and mantle-derived magmatism during the Laramide orogeny, in the mid-Tertiary, and continuing into the Neogene (e.g., 0–10-Ma volcanism along the Jemez lineament). In the Sandia Mountain region, these processes may be responsible for the approximately 1600 m of initial, pre-rift topography inferred from our flexural models.

CONCLUSIONS

A joint-inversion of topography and gravity data east of the northern Albuquerque basin suggests that the present-day topography of the Sandia Mountains is consistent with flexural rift-flank uplift in response to extension. The best-fitting plate flexure is of short wavelength, suggesting that the plate may have been locally weakened adjacent to the Rio Grande rift and that flexural responses are confined to within a short distance from the Rio Grande rift. However, the rift-flank uplift mechanism seems incapable of explaining the observed topographic variation along the flanks of the Rio Grande rift.

We propose that the broad, regional topographic high (Alvarado ridge) at the eastern margin of the Colorado Plateau probably pre-dated Rio Grande rift extension. Based on geologic and geomorphologic arguments, together with initial elevations estimated from our flexural analysis, we suggest that the present-day topography of Alvarado ridge represents regional (ongoing?) uplift that commenced prior to Rio Grande rift extension. Therefore, the present-day topographic setting of the Rio Grande rift and the eastern margin of the Colorado Plateau is a combined effect of the following sequence of uplift events: (1) Laramide crustal thickening (Cretaceous to Eocene); (2) regional epeirogeny and denudation (late Oligocene to early Miocene); and (3) short-wavelength rift-flank flexure associated with Neogene extension in the Rio Grande rift.

ACKNOWLEDGMENTS

We thank G. R. Keller for providing us with regional raw and reduced Bouguer gravity data for the Rio Grande rift and vicinity. This manuscript greatly benefited from reviews by J. Geissman and G. R. Keller. M. R. thanks the Caswell Silver Foundation for supporting her research at the University of New Mexico.

REFERENCES

Abbott, J. C., 1995, Constraints on the deformational history of the Tijeras-Canoncito fault system, north-central New Mexico [M.S. thesis]: Socorro, New Mexico Institute of Mining and Technology, 161 p.

Barrow, R. and Keller G. R., 1994, An integrated geophysical study of the Estancia basin, central New Mexico; *in* Keller, G. R. and Cather, S. M., eds., Basins of the Rio Grande rift: structure, stratigraphy, and tectonic setting: Geological Society of America, Special Paper 291, p. 171–186.

Block L. and Royden L. H., 1990, Core complex geometries and regional scale flow in the lower crust: Tectonics, v. 9, p. 557–567.

Broadhead, R. F., 1997, Subsurface geology and oil and gas potential of Estancia basin, New Mexico: New Mexico Bureau of Mines and Mineral Resources, Bulletin 157, 54 p.

Brown, C. D. and Phillips, R. J., 1997, Flexural rift-flank uplift at the Rio Grande rift: EOS, Transactions of the American Geophysical Union, v. 78, p. 321.

Chapin, C. E., 1971, The Rio Grande rift, part 1: Modifications and additions: New Mexico Geological Society, Guidebook 22, p. 191–201.

Chapin C. E. and Cather S. M., 1994, Tectonic setting of the axial basins of the northern and central Rio Grande rift; *in* Keller, G. R. and Cather, S. M., eds., Basins of the Rio Grande rift: Structure, stratigraphy, and tectonic setting: Geological Society of America, Special Paper 291, p. 5–25.

Chapin, C. E. and Kelley, S. A., 1997, The Rocky Mountain erosion surface in the Front Range of Colorado; *in* Bolyard, D. W. and Sonnenberg, S. A., eds., Geologic history of the Colorado Front Range: Rocky Mountain Association of Geologists, Symposium Guidebook, p. 101–114.

Chase, C. G., Gregory-Wodzicki, K. M., Parrish, J. T. and DeCelles, P. G., 1998, Topographic history of the Western Cordillera of North America and controls on climate; *in* Crowley, T. J. and Burke, K., eds., Tectonic boundary conditions for climate model simulations: Oxford Monographs on Geology and Geophysics, Oxford University Press, p. 73–99.

Eaton, G., 1986, A tectonic redefinition of the southern Rocky Mountains: Tectonophysics, v. 132, p. 163–193.

Evanoff, E., 1990, Early Oligocene paleovalleys in southern and central Wyoming: Evidence of high local relief on the late Eocene unconformity: Geology, v. 18, p. 443–446.

Evanoff, E., 1998, Geomorphic and stratigraphic evidence for late Cenozoic tilting of the Laramie Mountains, southeast Wyoming: Geological Society of America, Rocky Mountain Section, Abstracts with Programs, v. 30, p. 8–9.

Gregory, K. M. and Chase C. G., 1994, Tectonic and climatic significance of a late Eocene low-relief, high-level geomorphic surface, Colorado: Journal of Geophysical Research, v. 99, p. 20,141–20,160.

Humphreys, E. D. and Dueker K. G., 1994a, Western U.S. upper mantle structure: Journal of Geophysical Research, v. 99, p. 9615–9634.

Humphreys, E. D. and Dueker K. G., 1994b, Physical state of the Western U.S. upper mantle: Journal of Geophysical Research, v. 99, p. 9635–9650.

Jones, C. H., Unruh, J. R. and Sonder, L. J., 1996, The role of gravitational potential energy in active deformation in the southwestern United States: Nature, v. 381, p. 37–41.

Karlstrom, K. E. and Humphreys, E. D., 1998, Persistent influence of Proterozoic accretionary boundaries in the tectonic evolution of southwestern North America: Interaction of cratonic grain and mantle modification events: Rocky Mountain Geology, v. 33, p. 161–179.

Keller, G. R., Snelson, C. M., Sheehan, A. F. and Dueker, K. G., 1998, Geophysical studies of crustal structure in the Rocky Mountain region: A review: Rocky Mountain Geology, v. 33, p. 217–228.

Kelley, S. A., 1990, Late Mesozoic to Cenozoic cooling history of the Sangre de Cristo Mountains, Colorado and New Mexico: New Mexico Geological Society, Guidebook 41, p. 123–132.

Kelley, S. A., Chapin, C. E. and Corrigan, J., 1992, Late Mesozoic to Cenozoic cooling histories of the flanks of the northern and central Rio Grande rift, Colorado and New Mexico: New Mexico Bureau of Mines and Mineral Resources, Bulletin 145, 40 p.

Kelley, S. A. and Chapin, C. E., 1995, Apatite fission-track thermochronology of southern Rocky Mountain–Rio Grande rift–western High Plains provinces: New Mexico Geological Society, Guidebook 46, p. 87–96.

Kelley, S. A. and Chapin, C. E., 1997, Internal structure of the southern Front Range, Colorado, from an apatite fission-track thermochronology perspective; *in* Bolyard, D. and Sonnenberg, S. A., eds., Tectonic history of the Front Range: Rocky Mountain Association of Geologists, Symposium Guidebook, p. 19–30.

Kelley, V. C., 1975, Structural sections of the Sandia Mountain area, New Mexico: New Mexico Bureau of Mines and Mineral Resources, Memoir 29, Map 4.

Kelley, V. C. and Northrop, S. A., 1975, Geology of Sandia Mountain and vicinity, New Mexico: New Mexico Bureau of Mines and Mineral Resources, Memoir 29, 136 p.

Knight, S. H., 1953, Summary of the Cenozoic history of the Medicine Bow Mountains, Wyoming: Wyoming Geological Association Guidebook, Eighth Annual Field Conference, p. 65–76.

Kruse, S. and Royden L. H., 1994, Bending and unbending of an elastic lithosphere: the Cenozoic history of the Apennine and Dinaride foredeep basins: Tectonics, v. 13, p. 278–301.

Lachenbruch, A. H. and Morgan, P., 1990, Continental extension, magmatism, and elevation; formal relations and rules of thumb: Tectonophysics, v. 174, p. 39–62.

May, S. J., Kelley, S. A. and Russell, L. R., 1994, Footwall unloading and rift shoulder uplifts in the Albuquerque basin: Their relation to syn-rift fanglomerates and apatite fission-track ages; *in* Keller, G. R. and Cather, S. M., eds., Basins of the Rio Grande rift: Structure, stratigraphy, and tectonic setting: Geological Society of America, Special Paper 291, p. 125–134.

Menne, B., 1989, Structure of the Placitas area, northern Sandia uplift, Sandoval County, New Mexico [M.S. thesis]: Albuquerque, University of New Mexico: 163 p.

Pazzaglia, F. J. and Kelley, S. A., 1998, Large scale geomorphology and fission-track thermochronology in topographic and exhumation reconstructions of the southern Rocky Mountains: Rocky Mountain Geology, v. 33, p. 229–257.

Roy, M., Royden, L. H., Burchfiel, B. C., Tzankov, T. and Nakov, R., 1996, Flexural uplift of the Stara Planina range, central Bulgaria: Basin Research, v. 8, p. 143–156.

Russell L. R. and Snelson, S., 1994, Structure and tectonics of the Albuquerque basin segment of the Rio Grande rift: Insights from reflection seismic data; *in* Keller, G. R. and Cather, S. M., eds., Basins of the Rio Grande rift: Structure, stratigraphy, and tectonic setting: Geological Society of America, Special Paper 291, p. 83–112.

Sheehan, A. F., Abers, G. A., Jones, C. H. and Lerner-Lam, A. L., 1995, Crustal thickness variations across the Colorado Rocky Mountains from teleseismic receiver functions: Journal of Geophysical Research, v. 100, p. 20,391–20,404.

Turcotte, D. L. and Schubert, G., 1982, Geodynamics: Application of continuum physics to geological problems: J. Wiley and Sons, New York, 450 p.

Vening-Meinesz, F. A., 1950, Les 'grabens' africains, resultat de compression ou de tension dans la croute terrestre?: Bulletin of the Royal Colonial Institute of Belgium, v. 21, p. 539–552.

Wernicke, B. and Axen, G. J, 1988, On the role of isostasy in the evolution of normal fault systems: Geology, v. 16, p. 848–851.